ChemComm

COMMUNICATION

View Article Online
View Journal | View Issue

Cite this: *Chem. Commun.*, 2015, **51**, 5939

Received 6th February 2015,
Accepted 26th February 2015

DOI: 10.1039/c5cc01115a

www.rsc.org/chemcomm

Controlled cutting and hydroxyl functionalization of carbon nanotubes through autoclaving and sonication in hydrogen peroxide†

Ethan J. Weydemeyer,‡ Alicia J. Sawdon‡ and Ching-An Peng*

In this study, an eco-friendly process utilizing a low concentration of hydrogen peroxide along with autoclaving and sonication was developed, accomplishing both carbon nanotube size reduction and hydroxyl functionalization.

Pristine carbon nanotubes (CNTs) often have lengths in the range of tens of micrometers, prompting researchers to develop means to shorten the length of CNTs for various applications. Shortened nanotubes have gained increasing attention in various areas such as the development of organic photovoltaic devices, the exploitation of CNT transport properties, use as connectors for molecular electronic devices, and a multitude of biomedical applications.[1–8] While the potential of CNTs is vast, many of the aforementioned uses require CNTs to be sized in the nano-scale. In addition, due to their inherent hydrophobicity, CNTs must be modified for applications in which aqueous solubility is required.[9]

Several methods to shorten CNTs have been developed. Broadly, they can be categorized as either physical, electrical, or chemical approaches. Mechanical cutting involves direct application of shear and normal forces to sever CNTs.[10] Ball milling is typically employed to cut CNTs mechanically, and it can reduce CNT sizes to 100 nm at high throughput.[11] However, standard ball milling does not introduce any functional groups which significantly enhance water solubility or allow for subsequent functionalization reactions. Microlithography and reactive ion etching are two electrical approaches for CNT size reduction.[12,13] Both processes can cut CNTs with exemplary precision, and are excellent choices for constructing electronic devices from individual CNTs. Unfortunately, electrical methods do not innately create functional groups which enhance water solubility or serve as a platform for additional reactions. In addition, electrical methods are limited to cutting low volumes of nanotubes, and the equipment necessary for cutting is expensive. While physical and electrical methods offer numerous advantages, chemical approaches are the dominant high-throughput, economical methods for simultaneously achieving functionalization, size reduction, and water solubility of CNTs.

Perhaps the most widely adopted chemical approach for simultaneous cutting and aqueous solubilization is refluxing of CNTs in the presence of concentrated strong acids, most commonly a mixture of 90% H_2SO_4 and 70% HNO_3 in a 3 : 1 ratio.[14–17] Strong acid reflux leads to the formation of carboxylic acid functional groups, which improve water solubility and are a suitable platform for subsequent CNT surface modification. While effective, such a method draws safety concerns and produces hazardous wastes. Because of increased concern about the environment, it is desirable to develop an eco-friendly process with greener solvent than strong acid for the functionalization and shortening of CNTs.

Hydrogen peroxide, a free-radical oxidizer which generates non-toxic byproducts and leaves no chemical residue, would be an ideal substitute for the aforementioned reasons. This notion is the basis of our investigation in this study—we describe an effective way to functionalize and shorten CNTs in a solution of hydrogen peroxide (30%), through autoclaving followed by tip-sonication. CNT cutting with hydrogen peroxide has not been previously reported. Unlike previously discussed methods, this is a simple, straightforward method with reduced hazards and environmental consequences.

To evaluate the effect of hydrogen peroxide on the cutting of CNTs, autoclave time, sonication time and sonication power were examined by using a dynamic light scattering (DLS) device (*i.e.*, Zetasizer). The results from these studies are summarized in Table 1.

Duration of autoclaving was found to significantly impact the CNT cutting process. Samples with an absence of autoclaving demonstrated negligible size reduction even with sonication at 4 W up to 4 h. Particle size distributions as measured by the Zetasizer are given in Table 1 (rows 1–3). Here, sonication time and power were kept constant at 2 h and 4 W, respectively. The sample which underwent 1 h of autoclaving showed a CNT size range of 70–6000 nm and an average size of 1006 nm (Fig. S1A, ESI†). Samples with 3 h and 5 h of autoclaving had size ranges of 70–3000 nm and 70–1000 nm, and average sizes of 616 nm and 293 nm, respectively (Fig. S1B and C, ESI†). CNTs with no autoclaving

Department of Chemical Engineering, Michigan Technological University, Houghton, MI 49931, USA. E-mail: cpeng@mtu.edu; Fax: +1 906 487-3213; Tel: +1 906-487-2569

† Electronic supplementary information (ESI) available: Experimental details and DLS results. See DOI: 10.1039/c5cc01115a

‡ Equal contribution.

Table 1 Result compilation of varying parameters on size analysis of CNTs (mean ± SD, n = 3)

Autoclave time (h)	Sonication power (W)	Sonication time (h)	Average size[a] (nm)
1	4	2	1006 ± 341
3	4	2	616 ± 117
5	4	2	293 ± 33
3	4	1	750 ± 101
3	4	4	289 ± 33
3	12	2	445 ± 22
3	20	2	323 ± 5

[a] As determined by DLS.

were unable to be dispersed (Fig. S6, ESI†) for Zetasizer measurements. Increasing duration of autoclaving yielded a concurrent narrowing of the overall size range and reduction in average size. It was surmised that 3 h of autoclaving was sufficient for achieving CNTs in the nano-scale range and was chosen as the optimal autoclaving time for subsequent studies.

As can be seen from Table 1 (rows 4 and 5), increasing the sonication time significantly impacts CNT size. CNTs sonicated for 1 h were quite disperse, with a size range of 70–5000 nm and an average size of 750 nm (Fig. S2A, ESI†). At 2 h of sonication, DLS results yielded a CNT size range of 70–2000 nm and an average size of 616 nm (Fig. S2B, ESI†). Following 4 h of sonication, all CNTs were below 1000 nm in length, and the average size was 289 nm, the lowest of any trial (Fig. S2C, ESI†). CNTs tended to follow either Gaussian or slightly skewed distribution. It should be noted that although high size reduction is achieved, we do not claim any lower limit of CNT size as autoclaving and sonication durations are increased.

Given the same duration of sonication (2 h), samples with higher sonication powers demonstrated increased cutting of CNTs. From DLS, CNTs sonicated at powers of 12 W, and 20 W had average sizes of 445 nm, and 323 nm, respectively (Table 1 rows 6 and 7). Increases in sonication power resulted in narrowing of the size distribution, which indicates a reduction in polydispersity (Fig. S3A–C, ESI†). As can be seen from Table 1, despite a five-fold increase in sonication power between the 4 W and 20 W samples, which reduced CNT size from 616 to 323 nm, an additional 2 h of autoclaving led to an average size change from 616 nm (Table 1 row 2) to 293 nm (Table 1 row 3) under 4 W. This indicates that an additional 2 h of autoclaving provides a similar size change in CNTs as raising the power from 4 W to 20 W. Likewise, an additional 2 h of sonication resulted in an average size change from 616 nm (Table 1 row 2) to 289 nm (Table 1 row 5) under 4 W. For this reason, using a sonication power above 4 W is not viewed as necessary and efficient, and 4 W of sonication was selected in later studies.

It is worth mentioning that the size distributions determined by Zetasizer should not be interpreted as the lengths of individual CNTs. Instead, they correspond to the size distributions of CNT aggregates within solution. However, CNT length reduction and aqueous solubilization should decrease the size of these aggregates. While the previous trials establish a relationship between aggregate size and magnitude of functionalization parameters, these experiments alone are insufficient to prove that both CNT length reduction and hydroxyl functionalization occurs.

To confirm CNT length reduction, TEM imaging was conducted, and the results are given in Fig. 1. By visual inspection, the relative sizes of CNT aggregates from both DLS measurements and TEM imaging appear similar, although such a conclusion is difficult to draw given the sparseness of individual CNT aggregates. It can be readily seen that as durations of both autoclaving and sonication are raised, the lengths of individual CNTs decreases, and the CNTs begin to develop partially cut sidewalls (as indicated by arrows). This demonstrates that CNT length is affected by both autoclaving and sonication, and the reduction in aggregate size does not solely result from an increase in water solubility. Moreover, compared to TEM of pristine CNTs (Fig. S4, ESI†), CNTs with any amount of autoclaving or sonication appear to have a rougher exterior, possibly due to hydrogen peroxide treatment.

From the previous experiments, it would appear that both autoclaving and sonication in hydrogen peroxide are critical to obtaining size reduction. Samples which underwent only autoclaving or sonication separately experienced negligible cutting. As shown in Fig. S6 (ESI†), the CNTs were settled down to the bottom of the vials. CNTs exposed to some combination of the two processes, even if only for short durations, demonstrated aqueous solubility and noteworthy size reduction (to below 1 μm). From these observations, we postulate that autoclaving and sonication are involved in separate reaction steps. In particular, autoclaving may generate hydroxyl radicals which attack CNTs and induce "weak sites," which can appear due to autoclaving alone.

There is however, not enough functionalization and shortening for CNTs to suspend well after autoclaving alone. The unstable areas formed during autoclaving, are then cleaved during sonication, which leads to overall size reduction and the presence of more functional groups on the CNTs, enhancing their overall aqueous solubility. The aqueous solubility of pristine and treated CNTs is shown in Fig. S5 (ESI†). After three days, pristine CNTs, CNTs with 3 h of autoclaving, and CNTs with 3 h of autoclaving and 4 h of

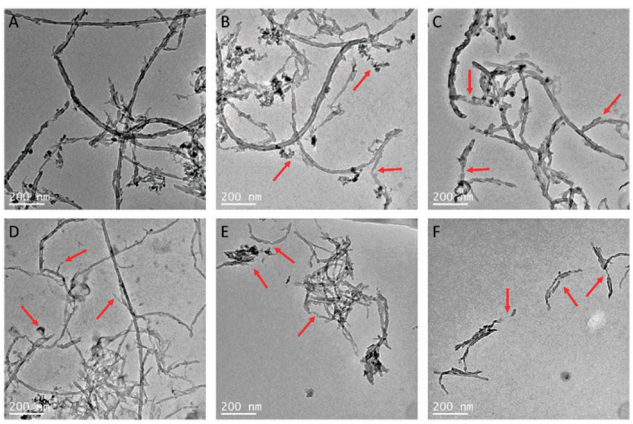

Fig. 1 TEM images of CNTs under varying autoclave and sonication time, power was kept constant at 4 W. Partially cut CNTs (shown by arrows). (A) 1 h autoclave time, 0 h sonication time; (B) 1 h autoclave time, 2 h sonication time; (C) 1 h autoclave time, 4 h sonication time; (D) 3 h autoclave time, 0 h sonication time; (E) 3 h autoclave time, 2 h sonication time; and (F) 3 h autoclave time, 4 h sonication time.

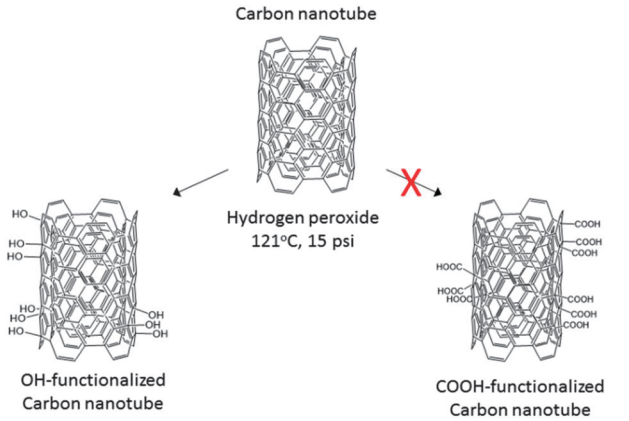

Fig. 2 Schematic representation of CNT functionalization. The potential mechanistic pathways of hydrogen peroxide treatment on CNTs are by way of hydroxyl or carboxyl groups. Through FTIR and ^{19}F NMR analyses, OH-functionalization was confirmed but not COOH-functionalization.

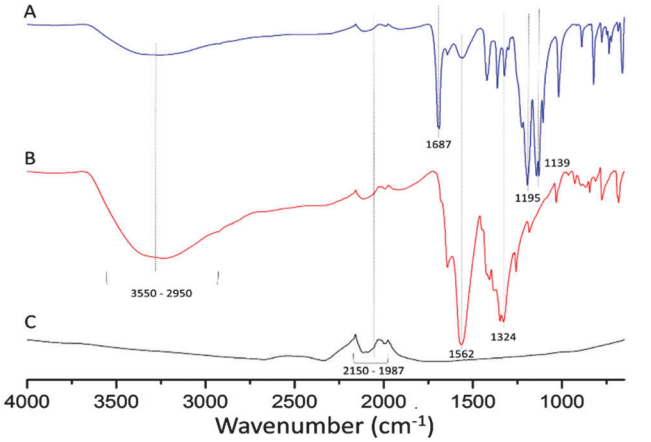

Fig. 3 FTIR spectra of (A) R_F-functionalized CNTs, (B) OH-functionalized CNTs, 3 h autoclave, 4 h sonication and (C) pristine CNTs.

sonication showed substantial differences in solubility. While autoclaving alone causes some suspension of CNTs, there is a much higher suspension in CNTs after both autoclaving and sonication.

Through TEM imaging, we noted that sidewall cutting of CNTs increased with increasing sonication duration. Therefore, we conclude that functional groups likely exist on the sidewalls of the CNTs, as their formation coincides with the CNT cutting. This is in contrast to the preferential appearance of functional groups on the ends of CNTs during cutting with sulfuric and nitric acid.[17] As can be seen from Fig. 2, it was hypothesized that autoclaving in hydrogen peroxide could yield two types of functionalization on the CNT surface, hydroxyl groups and carboxylic acid groups. This is because, as temperature is raised beyond 110–120 °C, hydrogen peroxide becomes unstable and decomposes spontaneously to hydroxyl radicals with the following reaction (1) and perhydroxyl radicals with the following reaction (2).[18]

$$H_2O_2 \rightarrow 2HO^{\bullet} \quad (1)$$

$$H_2O_2 \rightarrow HOO^{\bullet} + H^{\bullet} \quad (2)$$

However, with reaction (1) being the kinetically dominant reaction, most of generated hydroxyl radicals are expected to attack CNTs, leading to formation of hydroxyl groups on the CNT surface. An *ab initio* computational quantum mechanical study supports the functionalization of CNTs by hydroxyl radical adduct.[19] Besides OH radical addition to CNTs, it is speculated that some of highly active hydroxyl radicals produced from reaction (1) could trigger the following reaction (3) in aqueous H_2O_2 as the more dominant pathway than eqn (2) for the production of perhydroxyl radicals.

$$HO^{\bullet} + H_2O_2 \rightarrow HOO^{\bullet} + H_2O \quad (3)$$

Since the calculated barrier energies reveal that the OOH radical is much less reactive than the OH radical with regard to addition reactions with CNTs, cytosine, and thymine in both gas phase and aqueous media,[19,20] it is conjectured that the functionalization of CNTs through autoclaving in hydrogen peroxide will be mostly driven by hydroxyl radical addition.

To confirm the presence of hydroxyl functionalization on the CNT surface, FTIR and ^{19}F NMR analyses were employed. FTIR analysis revealed that we do indeed have hydroxyl group functionalization (Fig. 3B) on the CNT surface. The characteristic OH stretching from 2950–3550 cm^{-1} is seen in the CNTs autoclaved for 3 h in hydrogen peroxide and sonicated for 4 h at 4 W. Moreover, C–O stretching and C=C stretching were seen at 1324 and 1562 cm^{-1}, respectively. In addition, pristine CNTs exhibited bending vibrations from 1987–2150 cm^{-1}. It is surmised that this bending vibration belongs to the C=C bonds in the multiwalled CNTs (Fig. 3C). C=C IR frequency is typically between 1400–1600 cm^{-1}, the presence of a peak at 1562 cm^{-1} for the hydrogen peroxide treated sample (Fig. 3B) is believed due to the sonication of the CNTs. As shown in the TEM imaging, with increased sonication duration, the CNT surface becomes more rough, leading to breaks between C=C bonds. Forming both reactive sites for hydroxyl attachment and C=C bonds no longer in a rigid ring formation, which could account for the presence of the peak at 1562 cm^{-1}.

Absent in the FTIR spectra of the hydrogen peroxide treated CNTs is a peak for the carbonyl group of a carboxylic acid, despite the potential existence according to reactions (2) and (3). Therefore, to double confirm that there is indeed no carboxylic acid functionalization, functionalized CNTs were tried to label with Lucifer yellow *via* carbodiimide linker (1-ethyl-3-(3-dimethylaminopropyl) carbodiimide; EDC). Assuming the existence of carboxyl groups, EDC would react with both carboxyl groups on CNTs and amine groups on Lucifer yellow, leading to the formation of CNT-Lucifer yellow. After extensive washing, fluorescence spectroscopy was conducted on the final product. However, the fluorescence of Lucifer yellow was not detected (data not shown), indicating that either carboxyl groups do not exist on the functionalized CNTs, or they exist in a negligible amount.

Similarly, although the FTIR results suggest the presence of hydroxyl groups on functionalized CNTs, more rigorous confirmation of CNT functionalization was sought. To indirectly confirm the existence of hydroxyl groups, functionalized CNTs were allowed to react with perfluoro-octanoyl chloride. If hydroxyl groups were present, an esterification reaction would occur, leading to the formation of C_7F_{15}COO-CNT. Fig. S7 (ESI†) shows

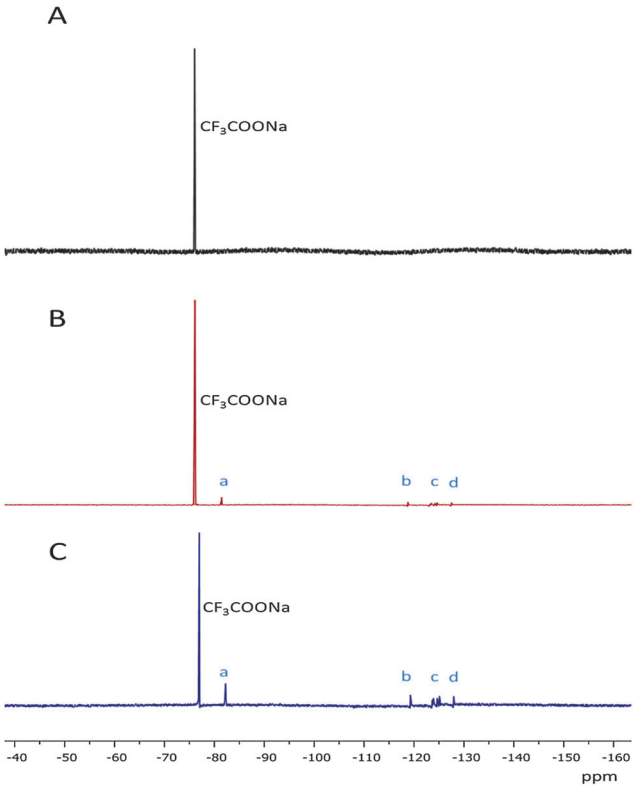

Fig. 4 ^{19}F NMR spectra of (A) pristine CNTs, (B) R_F-functionalized CNTs, 3 h autoclave, 0 h sonication and (C) R_F-functionalized CNTs, 3 h autoclave, 4 h sonication.

the esterification reaction scheme which was conducted on several types of CNTs: pristine CNTs, CNTs which underwent 3 h of autoclaving and 0 h sonication, and CNTs with 3 h of autoclaving and 4 h of sonication at 4 W. In the reaction, perfluoro-octanoyl chloride is reacted with suspected hydroxyl groups on the surfaces of cut CNTs. Hydrogen chloride generated from the reaction is scavenged by Na_2CO_3. In addition, this side reaction shifts the equilibrium reaction by Le Chatelier's principle to favor the formation of ester bonds between the CNTs and perfluoro-octanoyl chloride. As can be seen from Fig. 3A, the OH stretching vibration (2950–3550 cm^{-1}) in the perfluoro (R_F) functionalized CNT was decreased and there was the presence of prominent absorptions at 1687 (C═O), 1195 (CF_3) and 1139 (CF_2) cm^{-1} attributed to the R_F group bound to the CNTs through the esterification reaction. ^{19}F NMR was also performed as shown in Fig. 4. Here, pristine CNTs (Fig. 4A), R_F-functionalized CNTs with no sonication (Fig. 4B) and R_F-functionalized CNTs after 3 h sonication (Fig. 4C) were run separately through the esterification procedure using perfluoro-octanoyl chloride. Using CF_3COONa as an internal standard ($\delta = -76.03$), each spectrum was normalized. ^{19}F NMR revealed that pristine CNTs do not bind with perfluoroalkyl moieties (Fig. 4A) whereas the typical peaks at −82.35 (a-CF_3), −119.03 (b-CF_2), −123.28 to −125.36 (c-CF_2) and −127.69 (d-CF_2) were attributed to R_F-functionalization by perfluoro-octonoyl acid bound onto the CNT surface (Fig. 4B and C). The varying heights of the R_F groups were attributed to differing hydroxyl concentration on the CNT surface. This indicates that sonication provided additional hydroxyl groups on the CNTs, which increased the amount of reactive sites for conjugation with perfluoro-octanoyl chloride. However, due to the detection of perfluoroalkyl groups on CNTs with only autoclaving, we reason that hydroxyl groups are produced during autoclaving, although not enough groups are added to completely solubilize the CNTs. This coincides with our previous TEM images, which indicate that autoclaving without sonication yields partially cut and rough CNTs. Also, the CNTs treated by autoclaving alone did not suspend well as shown in Fig. S6 (ESI†).

The OH-functionalized CNT was further derivatized and conjugated with streptavidin-FITC (Fig. S8, ESI†) to indicate its potential applications with biotin-tagged matters.

In this study, we have determined that CNTs can be functionalized with hydroxyl groups through autoclaving and sonication in 30% hydrogen peroxide. Through FTIR and ^{19}F NMR analyses, a mechanistic pathway of OH-functionalization was determined and the existence of carboxylic acid functionalization absent. Moreover, prolonged exposure to high temperature and pressure conditions were found to increase the degree of CNT size reduction. Increases in tip-sonication duration and power level also led to greater cutting of the CNTs. This more eco-friendly and safety-conscious method of providing nano-sized CNTs with a novel functional group will hopefully give opportunities for further applications of CNTs in industry and a plethora of research areas.

This study was supported by the Michigan Tech Fund.

Notes and references

1 G. Kalita, S. Adhikari, H. R. Aryal, M. Umeno, R. Afre, T. Soga and M. Sharon, *Appl. Phys. Lett.*, 2008, **92**, 123508.
2 A. V. Eletskii, *Phys.-Usp.*, 2009, **52**, 209–224.
3 A. Aviram and M. A. Ratner, *Chem. Phys. Lett.*, 1974, **29**, 277–283.
4 G. Pastorin, W. Wu, S. Wieckowski, J.-P. Briand, K. Kostarelos, M. Prato and A. Bianco, *Chem. Commun.*, 2006, 1182–1184.
5 W. Yang, P. Thordarson, J. J. Gooding, S. P. Ringer and F. Braet, *Nanotechnology*, 2007, **18**, 412001.
6 B. S. Harrison and A. Atala, *Biomaterials*, 2007, **28**, 344–353.
7 A. Sawdon, E. Weydemeyer and C. A. Peng, *Eur. J. Nanomed.*, 2013, **5**, 131–140.
8 A. Bianco, K. Kostarelos and M. Prato, *Curr. Opin. Chem. Biol.*, 2005, **9**, 674–679.
9 G. Yu, M. Xue, Z. Zhang, J. Li, C. Han and F. Huang, *J. Am. Chem. Soc.*, 2012, **134**, 13248–13251.
10 P.-C. Ma, N. A. Siddiqui, G. Marom and J.-K. Kim, *Composites, Part A*, 2010, **41**, 1345–1367.
11 N. Pierard, A. Fonseca, Z. Konya, I. Willems, G. Van Tendeloo and J. B. Nagy, *Chem. Phys. Lett.*, 2001, **335**, 1–8.
12 S. R. Lustig, E. D. Boyes, R. H. French, T. D. Gierke, M. A. Harmer, P. B. Hietpas, A. Jagota, R. S. McLean, G. P. Mitchell and G. B. Onoa, *Nano Lett.*, 2003, **3**, 1007–1012.
13 T. Yuzvinsky, A. Fennimore, W. Mickelson, C. Esquivias and A. Zettl, *Appl. Phys. Lett.*, 2005, **86**, 053109.
14 T. Saito, K. Matsushige and K. Tanaka, *Phys. B*, 2002, **323**, 280–283.
15 K. J. Ziegler, Z. Gu, H. Peng, E. L. Flor, R. H. Hauge and R. E. Smalley, *J. Am. Chem. Soc.*, 2005, **127**, 1541–1547.
16 I. D. Rosca, F. Watari, M. Uo and T. Akasaka, *Carbon*, 2005, **43**, 3124–3131.
17 J. Liu, A. G. Rinzler, H. Dai, J. H. Hafner, R. K. Bradley, P. J. Boul, A. Lu, T. Iverson, K. Shelimov, C. B. Huffman, F. Rodriguez-Macias, Y. S. Shon, T. R. Lee, D. T. Colbert and R. E. Smalley, *Science*, 1998, **280**, 1253–1256.
18 R. Sundara, *Can. Chem. News*, 1998, **50**, 15–17.
19 A. Galano, *J. Phys. Chem. C*, 2008, **112**, 8922–8927.
20 A. Yadav and P. C. Mishra, *Int. J. Quantum Chem.*, 2013, **113**, 56–62.

